Heat Transfer in Squish Gaps

J.H. Spurk*
Technische Hochschule Darmstadt, Darmstadt, Federal Republic of Germany

It is shown that the flow in planar and annular squish gaps of internal combustion engines at the near end of the compression stroke resembles an unsteady stagnation point flow. When the ratio of the diffusion time across the boundary layer to the characteristic time of the outer flow is constant, as is the case when the final squish gap height is zero, then the compressible unsteady stagnation boundary-layer flow is self-similar. For a nonvanishing final gap height, the flow is nonsimilar but is treated locally in time as a quasisimilar flow. This quasisimilar flow may be computed by expanding the solution in powers of the above-mentioned ratio. The first term in this expansion is the steady compressible stagnation point boundary-layer flow. The reported heat-transfer rates have been measured in a single-stroke compression device. These agree well with only the first term in the expansion. Even steady incompressible stagnation point heat-transfer rates are found to correlate the experimental data satisfactorily.

Nomenclature

a = time function in Eq. (6)
A_c = cross-sectional area of the cylinder
C = constant in viscosity law ($\mu/\mu_\infty = CT/T_\infty$)
c_p = specific heat at constant pressure
f = dimensionless stream function
g = dimensionless temperature function
h = gap height
h_0 = final gap height at top dead center (TDC)
ℓ = gap width ($\ell = r_o - r_i$)
Nu = Nusselt number
p = pressure
Pr = Prandtl number
$\dot{q}$ = heat flux
r = variable
Re = Reynolds number
r_i = inner radius (half-width of recess channel in piston)
r_o = outer radius (half-width of piston)
s = stroke
t = time
T = temperature
T^+ = dimensionless wall temperature ($T^+ = T_w/T_\infty$)
u,v = velocity components in x and y directions
v_p = piston velocity ($v_p = \dot{h}$)
V_R = recess volume in piston
x = Cartesian coordinate along cylinder head
y = Cartesian coordinate normal to cylinder head
Y = material coordinate
γ = specific heat ratio
δ = boundary-layer thickness
ϵ = compression ratio
η = independent variable of similarity solution
λ = coefficient of thermal conductivity
μ = dynamic viscosity
ν = kinematic viscosity
ρ = density
τ = shear stress
ψ = stream function
ω = angular velocity

Superscripts

$(\dot{})$ = derivatives with respect to t ($\partial/\partial t$)
$(\,)'$ = derivatives with respect to η ($\mathrm{d}/\mathrm{d}\eta$)

Subscripts

w = wall conditions
∞ = conditions at outer edge of boundary layer

Introduction

HEAT transfer to the walls of the combustion chamber is one of the major losses in internal combustion engines. Its accurate prediction, therefore, is of some importance in the design and analysis of internal combustion engines. There are a large number of correlation formulas differing very appreciably in the prediction of the heat transfer.[1] The more successful correlations are based on steady turbulent pipe flow and the only geometric quantity entering these correlations is the piston diameter. It is obvious that such a correlation cannot properly account for truly time- and space-dependent heat transfer. It is most likely that an accurate prediction will have to await numerical computation of the whole three-dimensional flow in the engine.

In this paper, we are concerned with a particular aspect of the problem of heat transfer, namely the heat transfer in a squish gap, when the piston is nearing top dead center (TDC) on the compression stroke. We will consider only annular and planar squish gaps, but place emphasis on the plane gap, which is intrinsically more interesting and for most cases a good approximation for the annular gap. If the lateral extent of the squish gap is much larger than its height, which is the case near TDC, then the inviscid flow is similar to the well-known stagnation point flow. Since the flow develops practically from rest and since the pressure gradient is favorable until very close to TDC, the boundary layer can be expected to be laminar; of course, there may be residual turbulence from the intake process high enough to invalidate this assumption. The flow may even be considered quasi-steady for most of the interesting portion of its travel and, for modest accuracy requirements, the heat transfer may be obtained immediately from the known solutions for the heat transfer in steady flow.[2,3]

From the steady stagnation point boundary-layer solution, the boundary-layer thickness δ proportional to $(\nu/a)^{1/2}$, if $U_\infty = ax$ is the inviscid outer flow. Using this estimate, the time required for a change in the outer flow to diffuse across the boundary layer is $\delta^2/\nu = 1/a$ and its ratio to the characteristic time of the outer flow $U_\infty/(\mathrm{d}U_\infty/\mathrm{d}t) = a/\dot{a}$ is a measure of unsteadiness. For the boundary layer to react in a quasi-

Received April 8, 1986; presented as Paper 86-1331 at the AIAA/ASME Thermophysics and Heat Transfer Conference, Boston, MA, June 2-4, 1986; revision received June 25, 1986.

*Professor of Fluid Mechanics, Mechanical Engineering. Associate Fellow AIAA.

steady manner, the ratio $\dot{a}/a^2$ must be small.[4] The smallness of $\dot{a}/a^2$ would suggest that an expansion in the sequence $\dot{a}/a^2$, $\ddot{a}/a^3$, etc., is appropriate.

However, as the case $\dot{a}/a^2 = \frac{1}{2}$ shows, $\dot{a}/a^2$ is not the dominant ratio for most cases and, for this reason, a quasisimilar solution in a sense discussed below is better. Still, an expansion in powers of $\dot{a}/a^2$ is possible and we will construct an approximate solution based on the smallness of this ratio. Very near TDC, this solution becomes singular, since $\dot{a}/a^2 \to \infty$.

However, for the case of vanishing final squish gap height, the parameter $\dot{a}/a^2$ is constant and for this case an exact solution of the unsteady boundary layer is possible, as has been shown by Schuh for incompressible flow.[5] We extent this solution to compressible, but low Mach number flow. This exact solution also provides convenient checks in the approximate solution. We will also compare the theoretical predictions with heat-transfer measurements in a one-stroke square piston device. The comparison will show that the experimental data can be adequately correlated using the steady-state incompressible flow heat-transfer rates.

Inviscid Flow

We consider the configuration depicted in Fig. 1, where the piston moves in the negative y direction and where the distance $h(t)$ of the moving piston to the cylinder head is given as

$$h(t) = h_0 + \frac{s}{2}[1 - \cos(\omega t)] \tag{1}$$

Time $t=0$ corresponds to TDC and we restrict our analysis to $\omega t < 0$ and to $|\omega t| \ll 1$, i.e., to the compression stroke as the piston is nearing TDC. Only during this portion of the cycle is the squish gap effective.

For the density $\rho(t)$, assumed uniform in the chamber (since all velocities are small compared to the speed of sound and the acoustic transit time is much smaller than the characteristic time $1/\omega$), there follows from conservation of mass in the cylinder the equation

$$\frac{\rho(t)}{\rho(0)} = \frac{1 + A_c h_0/V_R}{1 + (A_c/V_R)[h_0 + s/2(1-\cos\omega t)]} \tag{2}$$

and for the temperature, from the assumption of isentropic flow:

$$\frac{T(t)}{T(0)} = \left[\frac{\rho(t)}{\rho(0)}\right]^{\gamma-1} \tag{3}$$

The characteristic time of the density $\rho/\dot{\rho}$ and of the temperature $T/\dot{T}$ are then proportional to $\sin\omega t \sim \omega t \ll 1$ and, as $t \to 0$, the temperature and the density enter the analysis with only their quasisteady values.

If the velocity in y direction is now taken as $V = (y/h)v_p$ (which satisfies the boundary condition at the piston and at the cylinder head), the x component of the velocity for the annular gap follows from the continuity equation,

$$U = -\frac{(r_o + r)(r_o - r)}{2r}\frac{v_p}{h} \tag{4}$$

and, as r_o and $r \to \infty$ with $r_o - r = x$ fixed, we get the U velocity for the planar gap,

$$U = -\frac{x}{h}v_p \tag{5}$$

Thus, the velocity field for the planar gap is that of an unsteady stagnation point flow. Equivalent to the assumption on V would have been the assumption that U is uniform at the exit ($x = \ell$). Of course, here a boundary condition on the pressure would have been more appropriate. But, it is obvious from the velocity distribution that the pressure is uniform at the exit up to terms of the order $(h/\ell)^2$. We have from Eqs. (1) and (5)

$$U = -\frac{\dot{h}}{h}x = a(t)x, \quad t < 0 \tag{6}$$

and the ratio of local to convective acceleration is

$$\frac{\dot{a}}{a^2} = \frac{\dot{h}^2 - \ddot{h}h}{\dot{h}^2} = \frac{1}{2} - \frac{2h_0/s}{\omega^2 t^2} + 0(\omega^2 t^2) \tag{7}$$

This is also the characteristic ratio for the boundary layer to adjust to the changing condition. For $|\dot{a}/\dot{a}^2| \ll 1$, the outer flow and the boundary-layer flows may be considered quasisteady. Typically, for $h_0/s = 10^{-2}$ and $8 < |\omega t| < 30$ deg (30 deg before TDC being the limit where the theory is applicable), $\dot{a}/a^2$ varies between -0.52 and 0.42. For $t \to 0$, the flow is always unsteady.

Boundary-Layer Flow

We restrict ourselves to boundary-layer flow for the planar gap. This case is a good approximation even for the annular gap, if $r_o r_i$ is sufficiently close to unity. Moreover, the experiments to be discussed were taken using a planar gap. In the limit that $h_0/s \to 0$, and for constant $\dot{a}/\dot{a}^2$, the boundary-layer equations admit a similarity solution, as has been shown by Schuh[5] and Yang.[6] For compressible flow, we use the boundary-layer equations as given by Stewartson,[7] but omit the dissipated energy and the work term in the energy equation (consistent with the assumption of low Mach number). We point out that in our case the boundary layer differs in one detail from the boundary layer near a stagnation point, since in viscous flow we should impose vanishing velocity on the line $x = 0$. In what follows, this boundary condition is ignored. If

$$Y = \int_0^y \frac{\rho}{\rho_\infty}\mathrm{d}y \tag{8}$$

$$\frac{\rho}{\rho_\infty}u = \frac{\partial\psi}{\partial y} \tag{9}$$

$$\frac{\rho}{\rho_\infty}v = -\frac{\partial\psi}{\partial x} - \frac{\partial Y}{\partial t} \tag{10}$$

we have for the equation of motion,

$$\frac{\partial^2\psi}{\partial Y\,\partial t} + \frac{\partial\psi}{\partial Y}\frac{\partial^2\psi}{\partial x\,\partial Y} - \frac{\partial^2\psi}{\partial Y^2}\frac{\partial\psi}{\partial x} = -\frac{T}{T_\infty}\frac{1}{\rho_\infty}\frac{\partial p}{\partial x} + v_\infty C\frac{\partial^3\psi}{\partial Y^3} \tag{11}$$

and for the energy equation

$$\frac{\partial T}{\partial t} + \frac{\partial\psi}{\partial Y}\frac{\partial T}{\partial x} - \frac{\partial\psi}{\partial x}\frac{\partial T}{\partial Y} = \frac{v_\infty C}{Pr}\frac{\partial^2 T}{\partial Y^2} \tag{12}$$

Here we have assumed a linear viscosity law, such that $\mu T_\infty = C\mu_\infty T$ and the Prandtl number $Pr = \mu c_p/\lambda$ and c_p to be constant. In Eqs. (11) and (12), the partial derivatives with respect to x are taken at constant Y and the reference conditions are those outside the boundary layer.

Similarity Solution

Using Eq. (6) and the new independent variable

$$\eta = Y\left[\frac{a(t)}{v_\infty C}\right]^{1/2} \tag{13}$$

and writing

$$\varphi = [a(t)v_\infty C]^{1/2} x f(\eta) \tag{14}$$

$$g(\eta) = (T - T_\infty)/(T_w - T_\infty) \tag{15}$$

Eqs. (11) and (12) are transformed into

$$\frac{\dot{a}}{a^2}\left(f' + \frac{\eta}{2}f''\right) + f'^2 - f''f$$

$$= \left[\frac{\dot{a}}{a^2} + 1\right]\left[1 - g\left(1 - \frac{T_w}{T_\infty}\right)\right] + f''' \tag{16}$$

and

$$\frac{\dot{a}}{a^2}\frac{\eta}{2}g' - g'f = Pr^{-1}g'' \tag{17}$$

The boundary conditions

$$u(x,0) = v(x,0) = 0, \quad u(x,\infty) = ax \tag{18}$$

and

$$T(x,0) = T_w, \quad T(x,\infty) = T_\infty = \text{const} \tag{19}$$

are written in the transformed variables as

$$f(0) = f'(0) = 0, \quad f'(\infty) = 1 \tag{20}$$

$$g(0) = 1, \quad g(\infty) = 0 \tag{21}$$

The shear stress at the wall and the heat transfer are now obtained as

$$\tau_w = \mu_w \frac{\partial u}{\partial y}\Big|_w = \rho_{1/2} a x (a v_\infty C)^{1/2} f''(0) \tag{22a}$$

and

$$\dot{q} = -\lambda_w \frac{\partial T}{\partial y}\Big|_w = -\lambda_w (T_w - T_\infty)\left(\frac{a}{v_\infty C}\right)^{1/2} g'(0) \tag{22b}$$

or in dimensionless form and referred to the wall conditions as

$$\frac{\tau_w}{\rho_w U_\infty{}^2} = \left[Re_w\left(\frac{x}{\ell}\right)^2\right]^{-1/2} f''(0), \quad Re_w = \frac{a\ell^2}{v_w} \tag{23a}$$

$$\frac{\dot{q}\ell}{\lambda_w (T_w - T_\infty)} = Nu_w = (Re_w)^{1/2}[-g'(0)] \tag{23b}$$

The velocity associated with the equation $\dot{a}/a^2 = \text{const}$ follows from integrating it, as

$$u = -x/(\dot{a}/a^2 t + c), \quad t < 0 \tag{24}$$

where the integration constant $c = 0$ because $u \to \infty$ as $t \to 0$.

In order to exhibit the effect of compressibility and of unsteadiness, the velocity profiles from the numerical solution of Eq. (16) for steady and unsteady flow are compared in Fig. 2 for two dimensionless wall temperatures $T^+ = 0$ and 2.

Because it acts through its addition to the pressure gradient, the unsteadiness influences the velocity profiles in a way known from the steady flow solutions.[3] For a heated wall, the flow is accelerated more in the hotter, lower-density portion of the boundary layer, which leads to an overshoot in the velocity and a thinner boundary-layer thickness in the transformed plane. However, in the physical plane, the boundary layer is thicker. For the cold wall, the flow in the denser portion of the boundary layer is accelerated less, leading to flatter profile and a larger boundary-layer thickness. We also consider negative values of $\dot{a}/a^2$. For $\dot{a}/a^2 = -1/2$ in Fig. 2, we observe that the flow near the hot wall is decelerated more than further away. In the cold-wall case, the velocity profile shows less deceleration near the wall, i.e., an acceleration when compared to steady flow. Briefly, the effect of acceleration of the main flow brings the profiles for $T^+ = 2$ and 0 further apart; that of deceleration brings the profiles closer together. In fact, for $\dot{a}/a^2 = -1$, the velocity profiles [and the profiles for $\rho(\eta)$] are the same for all wall temperatures, as Eqs. (16) and

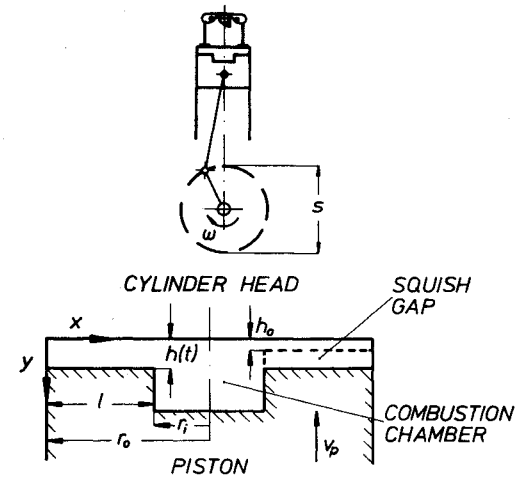

Fig. 1 Sketch of geometry.

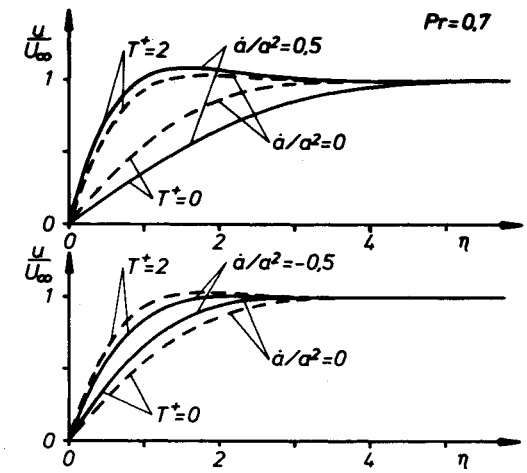

Fig. 2 Velocity profiles.

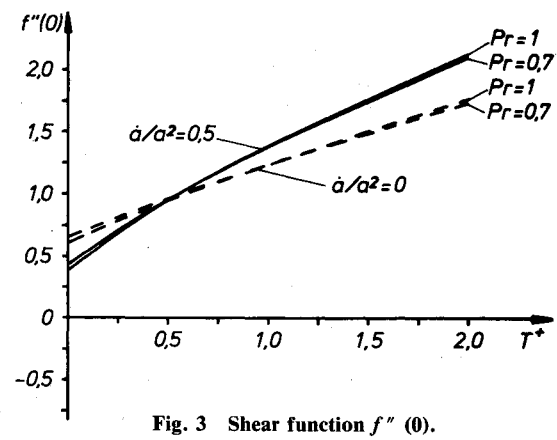

Fig. 3 Shear function $f''(0)$.

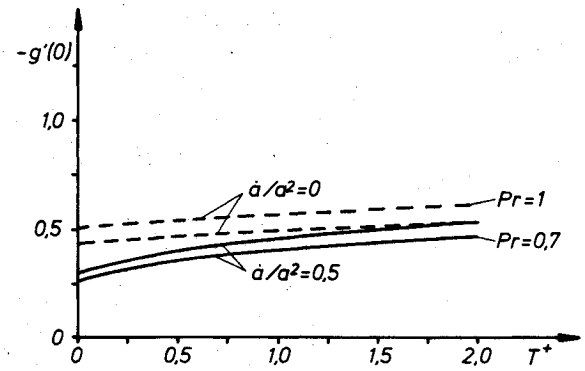

Fig. 4 Heat function $g'(0)$.

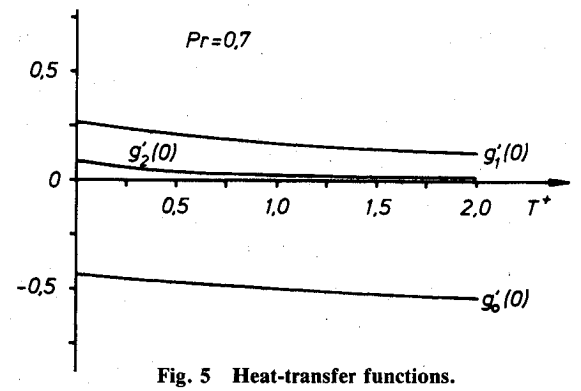

Fig. 5 Heat-transfer functions.

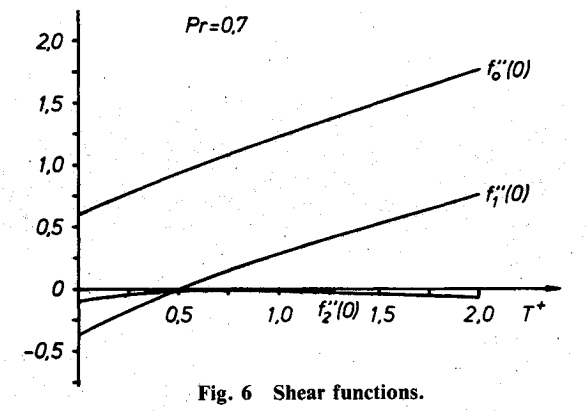

Fig. 6 Shear functions.

(17) show. This case is somewhat analogous to the flat-plate case in steady flow; of course, the remaining unsteady terms still affect the differences.

In Fig. 3, the shear function on the wall $f''(0)$ and, in Fig. 4, the heat-transfer function $g'(0)$ are compared for the practically important cases $\dot{a}/a^2=0$ and ½, i.e., $2h_0/s=0$. The effect of unsteadiness is to increase the shear function and the effect of compressibility is to do the same if $T^+>1$. For $T^+<1$, the compressibility decreases the shear. As far as the heat-transfer function $g'(0)$ is concerned, the effect of unsteadiness is to decrease the heat transfer, an effect that increases with decreasing wall temperature.

Perturbation Solution

For nonvanishing h_0/s, the flow is nonsimilar and, in general, must be computed solely by numerical methods.[8] But since h_0/s is small, we assume that the actual flow goes through a sequence of unsteady flows with the "local" value of $\dot{a}/a^2$ at time t. This procedure ignores all of the characteristic times except $a/\dot{a}$ that can be formed with $a(t)$,

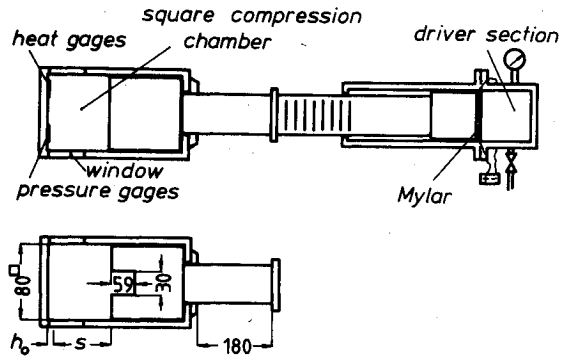

Fig. 7 Single-stroke compression engine (dimension in millimeters).

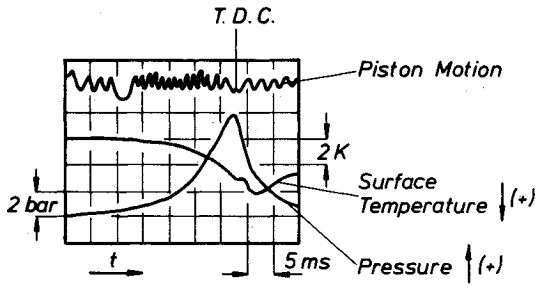

Fig. 8 Typical record.

but it is exact if $h_0/s\to 0$ and serves as basis for the perturbation solution to be discussed presently. Equation (24) may be considered as the velocity consistent with the local value of $\dot{a}/a^2$ when the integration constant c is determined from the actual velocity at time t. When $|\dot{a}/a^2|$ is small compared to unity, which is the case for most of the piston's travel, rather than to solve Eqs. (16) and (17) for the sequence of $\dot{a}/a^2$, we expand f in powers of $\dot{a}/a^2$. Accordingly, we put

$$f=f_0+\frac{\dot{a}}{a^2}f_1+\left(\frac{\dot{a}}{a^2}\right)^2 f_2+\ldots \tag{25}$$

$$g=g_0+\frac{\dot{a}}{a^2}g_1+\left(\frac{\dot{a}}{a^2}\right)^2 g_2+\ldots \tag{26}$$

If Eqs. (25) and (26) are inserted into Eqs. (16), (17), (20), and (21), we obtain the following system:

$$f_0'^2-f_0''f_0=f_0'''+1-g_0(1-T_w/T_\infty) \tag{27a}$$

$$-g_0'f_0=\frac{1}{Pr}g_0'' \tag{27b}$$

$$f_0(0)=f_0'(0)=0;\ f_0'(\infty)=1 \tag{28a}$$

$$g_0(0)=1;\ g_0(\infty)=0 \tag{28b}$$

further

$$f_0\frac{\eta}{2}+f_0'+2f_0'f_1'-f_1'f_0''-f_0f_1''$$
$$=f_1'''+1-(g_0+g_1)(1-T_w/T_\infty) \tag{29a}$$

$$g_0'\frac{\eta}{2}-g_0'f_1-g_1'f_0=\frac{1}{Pr}g_1'' \tag{29b}$$

$$f_1(0)=f_1'(0)=f_1'(\infty)=0 \tag{30a}$$

$$g_1(0)=g_1(\infty)=0 \tag{30b}$$

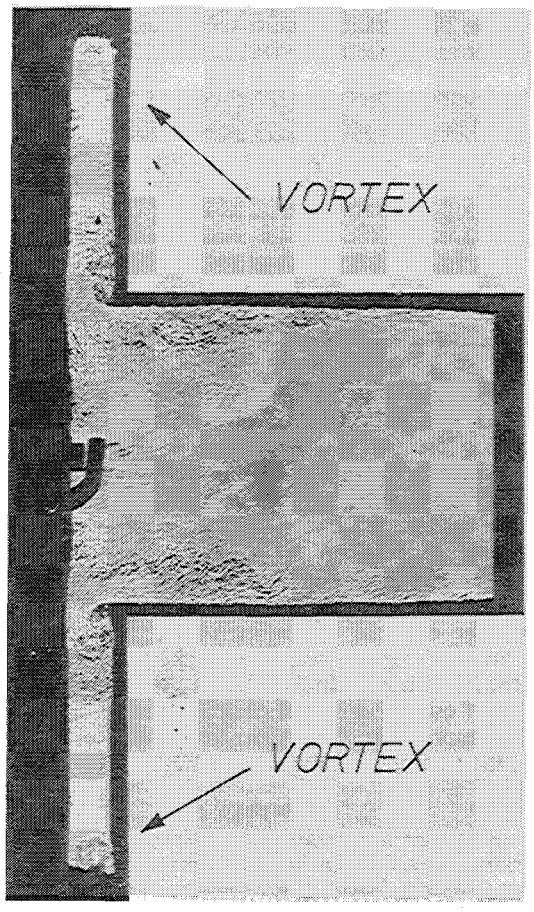

Fig. 9 Shadowgraph of squish gap flow.

and

$$f_1' + \frac{\eta}{2} f_1'' + 2f_2' f_0' + f_1'^2 - f_0'' f_2 - f_0 f_2'' - f_1'' f_1$$

$$= f_2''' - (g_1 + g_2)(1 - T_w/T_\infty) \tag{31a}$$

$$\frac{\eta}{2} g_1' - g_2' f_0 - g_0' f_2 - g_1' f_1 = \frac{1}{Pr} g_2'' \tag{31b}$$

$$f_2(0) = f_2'(0) = f_2'(\infty) = 0 \tag{32a}$$

$$g_2(0) = g_2(\infty) = 0 \tag{32b}$$

The system of Eqs. (27) is the same as Eqs. (16) and (17), if there $\dot{a}/a^2$ is set to zero, i.e., it describes the steady flow. The numerical solution of Eqs. (27–32) has been compared with the exact solutions of Eqs. (16) and (17) for various values of $\dot{a}/a^2$, with the result that for $\dot{a}/a^2 = -\frac{1}{2}$ the difference between the exact and the perturbation solution is 1% in $f''(0)$ and $g'(0)$ for a cold wall and less for the other wall temperatures. For $\dot{a}/a^2 = \frac{1}{2}$, the error rises to 6% in $g'(0)$ and 5% in $f''(0)$, again for the cold wall and less than 2% for the other cases. Values of $\dot{a}/a^2 > \frac{1}{2}$ are not of interest in this context, but it is worth pointing out that numerical difficulties were encountered for $\dot{a}/a^2 \geq 1$ and $T^+ = 0$, where the finite-difference solution of the boundary value problem did not agree with routinely made recomputation as an initial value problem. An asymptotic analysis suggests that no solution of the system (16–19) exists for $\dot{a}/a^2 > 2$. For negative $\dot{a}/a$, no difficulties were encountered in the range considered and the error of the perturbation solution was found to be 5% in $g'(0)$ and $f''(0)$ even for $\dot{a}/a^2 = -1$; here the error is the same for all wall temperatures. Thus, with the aid of Figs. 5 and 6, the heat transfer and shear stress may now be estimated for $\dot{a}/a^2$ in range -1.0 to 0.5 from Eq. (23b).

For values smaller than -1.0, one should solve Eqs. (16) and (17). There will be hardly any need for it, since Eq. (23b) shows the heat transfer to be proportional to $(Re_w)^{1/2}$. The maximum of Re_w is reached for $\omega t = (4h_0/s)^{1/2}$, typically ~ 11 deg before TDC. This corresponds to $\dot{a}/a^2 = 0$, while $\dot{a}/a^2 = -1$ corresponds to 6 deg before TDC. If only the largest value of the heat transfer is of interest, then in the quasisimilar approximation one may simply use the steady heat-transfer rates. As $Re_w \to 0$, the heat transfer is by conduction and the rates are usually much smaller than the convection rates. For strong deceleration, reverse flow will occur near the wall; for incompressible flow, Yang[9] found $f'(0) = 0$ at $\dot{a}/a^2 = -3.175$. For the cold wall, we expect that any flow reversal will be delayed.

Experiments

The heat transfer has been measured using thin-film gages mounted in the head of a single-stroke cylinder-piston device,[10] as shown schematically in Fig. 7. The heat gage was calibrated in a shock tube by relating the measured resistance change to the computed surface temperature behind a reflected shock wave. Various tests gave a scatter of $\pm 10\%$ in the calibrating constant.

The square piston is driven by a push rod connected to a piston in the driver section. Initially, the driver piston is separated from a high-pressure driver section by a Mylar membrane; also, the pressure and temperature in the cylinder have their atmospheric values.

A thin wire is passed over the membrane, which ruptures when the wire is suddenly heated. The driver piston then pushes the working piston into the cylinder, compressing the gas in the cylinder. The motion of the piston and the pressure are recorded. The square cylinder has plane windows in the side walls that allow observation of the flow. The square working piston has a channel-like recess, such that two symmetrical planar squish gaps are formed when the piston approaches the cylinder head. The resistance of the thin-film gage is measured as a function of time, allowing the surface temperature to be determined. This surface temperature is reduced to heat-transfer data and immediately compared to Eq. (23b).[11] In addition to the heat-transfer measurements, shadowgraph pictures at various distances of the piston from TDC and high-speed movies with 8000 frames/s were taken.

Results

Figure 8 is a typical oscillogram showing the surface temperature (positive down) and pressure (positive up) history during compression and expansion. The upper trace is an output from an induction gage that senses the passage of equidistantly spaced conducting strips on the push rod. Two subsequent maxima of the signal correspond to a known advance of the rod. TDC is recognized as a phase shift of the signal. The surface temperature reaches a maximum near TDC and then drops, rising again during the expansion; this temperature actually achieves higher values during expansion than during compression.

This secondary rise is not easily reproduced and the visual observation suggests that it is connected with transition to turbulent flow in the gap. The frame picture in Fig. 9, taken shortly after TDC, gives an impression on how this happens.

At the beginning of the downstroke, the turbulence formed during compression in the wakes of the flow separating at the exit corners is "sucked" into the gap. As the motion pictures show, at the same time vortex-like structures appear to move out of the corners (between the cylinder head and sidewalls) and through the gap to the exit. In their wake, the flow is turbulent. They can be seen in the frame picture (Fig. 9) in a position still close to the outside walls. The spatial resolution of the motion picture does not allow identification of the cause for these structures. One hypothesis is that, at the beginning of

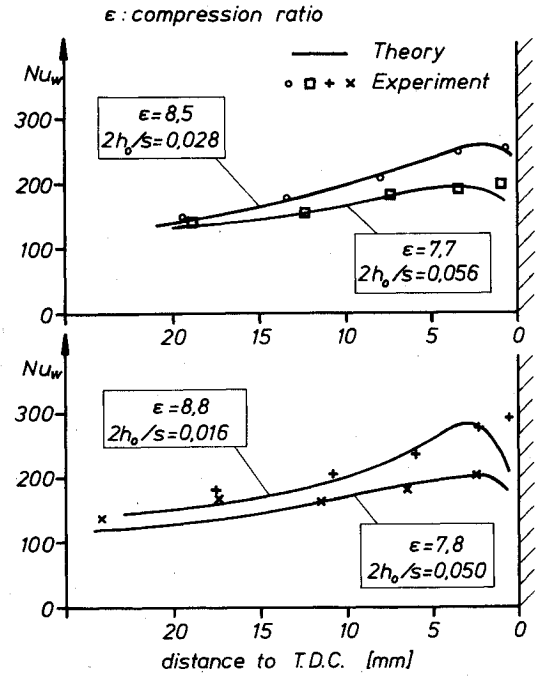

Fig. 10 Comparison of measured Nusselt number with theory for steady flow.

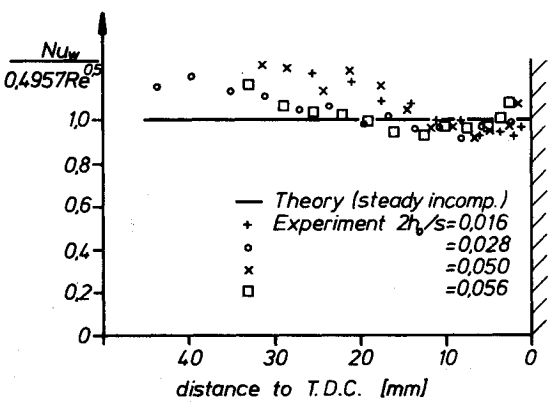

Fig. 11 Experimental heat-transfer rates compared with theory for steady incompressible flow.

the downstroke, there is a backflow from crevices which gives rise to the vortex-like structures. The other is that vortices are formed in the corner (as one would expect) during the quasisteady portion of the flow. These are held in the corners by the convection field until the velocity tends to zero, when they must move (in order to satisfy the boundary condition at the walls). If this hypothesis is correct, the phenomenon will also occur in an actual engine and constitute an effective mechanism for rendering the flow turbulent in the gap. Figure 8 also shows that leakage is quite severe since peak pressure is reached not at, but before, TDC.

Comparison between Theory and Experiment

The motion of the piston $h(t)$ was obtained from the upper trace in Fig. 8. Note that here the motion is determined by the dynamics of the compression device and not fixed by the kinematics of the crank action, as is the case in an engine. Therefore, some of the specific remarks made earlier do not apply here. In Fig. 10, the measured Nusselt number is compared with theoretical predictions.

The theoretical curves apply to compressible *steady* flow, i.e., $\dot{a}/a^2 = 0$. The measured motion $h(t)$ was not accurate enough to extract the acceleration $\ddot{h}(t)$ needed for evaluation of the actual $\dot{a}/a^2$ from Eq. (7). Various fits to the experimental $h(t)$ gave widely differing values for $\dot{a}/a^2$. However, all the fits showed values of $\dot{a}/a^2$ approximately zero near TDC, so that a comparison with this value seems most appropriate. The predicted value may then be too high further away from TDC. The agreement between theory and experiment is quite good, even at distances up to 25 mm, where $h/\ell \sim 0(1)$ and the theory is hardly applicable. It would appear that this is due to the compensating effects by assuming steady flow and violating the essential condition $h/\ell \ll 1$. Nevertheless, the agreement is also good near TDC, where $\dot{a}/a^2 \approx 0$ and the above condition is met. In Fig. 11, we give a comparison between all of our experimental data and the theory based on steady incompressible flow. Apart from distances larger than 25 mm, the data are correlated quite well.

References

[1]Pflaum, W. and Mollenhauer, K., *Warmeübergang in der Verbrennungsmaschine*, Springer-Verlag, Vienna and New York, 1977.

[2]Cohen, C.B. and Reshotko, E., "Similar Solutions for the Compressible Laminar Boundary Layer with Heat Transfer and Pressure Gradient," NACA Rept. 1923, 1956.

[3]Moore, F.K. (ed.), *Theory of Laminar Flow: High Speed Aerodynamics and Jet Propulsion*, Vol. IV, Princeton University Press, Princeton, NJ, 1964.

[4]Moore, F.K., "Unsteady Laminar Boundary Layer Flow," NACA TN 2471, 1951.

[5]Görtler, G. and Tollmien, W. (eds.), *50 Jahre Grenzschichtforschung*, Friedrerick Vieweg & Sohn, Braunschweig, FRG, 1955.

[6]Yang, K.T., "Unsteady Laminar Boundary Layers in an Incompressible Stagnation Flow," *Journal of Applied Mechanics*, Vol. 25, 1958, pp. 421-427.

[7]Stewartson, K., "On the Impulsive Motion of a Flat Plate in an Viscous Fluid," *Quarterly Journal of Mechanics and Applied Mathematics*, Vol. IV, Pt. 2, 1951, pp. 182-198.

[8]Vimala, B.C. and Nath, G., "Unsteady Laminar Boundary Layers in a Compressible Stagnation Flow," *Journal of Fluid Mechanics*, Vol. 70, Pt. 3, 1975, pp. 561-572.

[9]Yang, K.T., "Unsteady Laminar Boundary Layers over an Arbitrary Cylinder with Heat Transfer in an Incompressible Flow," *Journal of Applied Mechanics*, Vol. 26, June 1959, pp. 171-178.

[10]Spengel, C. and Müller, M., "Experimenteller Nachweis des Warmeüberganges in der Verdrängungsströmung eines Quetschspaltes," Studienarbeit Technische Strömungslehre, Technische Hochschule Darmstadt, Darmstadt, FRG, 1985.

[11]Schultz, D.L. and Jones, T.V., "Heat Transfer Measurements in Short-Duration Hypersonic Facilities," AGARD AG 165, 1973.